

Release Lanyard Design

By:

Andrew Baker, Tim Haynes, Styson Koide,
David Lofgreen, Carly Siewerth and Chris Temme
Team05

Document

Final Report

*Submitted towards partial fulfillment of the requirements for
Mechanical Engineering Design – Spring 2013*



Department of Mechanical Engineering
Northern Arizona University
Flagstaff, AZ 86011

Table of Contents

Introduction	Page 2
Needs Identification	Page 2
Project Goals	Page 2
Constraints	Page 2
Objectives	Page 3
Current Internal Components.....	Page 3
Preliminary Designs.....	Page 4
Design Analysis and Modifications.....	Page 5
New Base Plate Design.....	Page 7
Material Selection.....	Page 8
Top Designs	Page 10
Testing.....	Page 16
Project Plan.....	Page 21
Conclusion	Page 21
References.....	Page 23

Introduction

Many weapons constructed by Raytheon use a lanyard to activate the weapon after it has been released. Unfortunately on a few occasions the lanyard has failed to activate the weapon due to icing, poor installation, and contaminants such as sand and dust. Raytheon has proposed this project to our team to create a new design that is more reliable and less susceptible to these modes of failure.

Needs Identification

This project consisted of developing a new design for an arming system lanyard and a functional prototype. The current lanyard design did not address issues relating to extreme temperatures and environmental effects, which led to system malfunction.

Project Goal

Our goal was to design a reliable, low cost system that could withstand extreme temperatures and environmental effects. This system was also constrained due to size and specific material requirements.

After a meeting on January 10, 2013 with Raytheon's release lanyard design supervisors, the emphasis of our design analysis changed to focus primarily on the internal activation mechanism, instead of the external components. This changed the original design problem from redesigning an entire lanyard system to redesigning the slider switch assembly, which disregarded the cable, cable guide components, and activation arm.

Constraints

- i. The device had to fit within the dimensions of the environmental testing chamber, which can simulate conditions that the current design is failing under.
- ii. The placement of the lanyard mounts and associated devices such as the battery had already been predetermined.
- iii. Internal components had to fit in the allowable housing space.
- iv. Internal activation switches could not be modified.
- v. The allowable cost could not exceed that of the current design which was \$300 in material cost.
- vi. Must be easily assembled within 30 minutes.

Objectives

With the information provided to us by our client, we constructed the following table based on the most important criteria.

Table 1: Objectives

Objectives	Basis for Measurement	Units
Inexpensive	Manufacturing Cost Based on Current Design	\$300
Maintain Current Location of Devices	Location Based on Current Design	Meters
Installation and Assembly	Timed Trial	Seconds
Successful Activation of Devices	Minimum Force Required	Newton's
Low Susceptibility to Contamination	Amount of Contamination Required to Induce Failure	Kilograms
High Performance Reliability	Number of Successful Attempts vs. Failed	%

Current Internal Components

As mentioned in the introduction, the current lanyard design failed to activate the weapon due to icing, poor installation, and contaminants such as sand and dust. The exact location of the icing or debris build up was unknown, but resulted in the cable breaking at the fuseable link prior to activation. The current slider design can be found in the Figure 1 below. One of the primary issues upon seeing the internal components of the activation system was the complexity and surface area for ice and debris to accumulate.

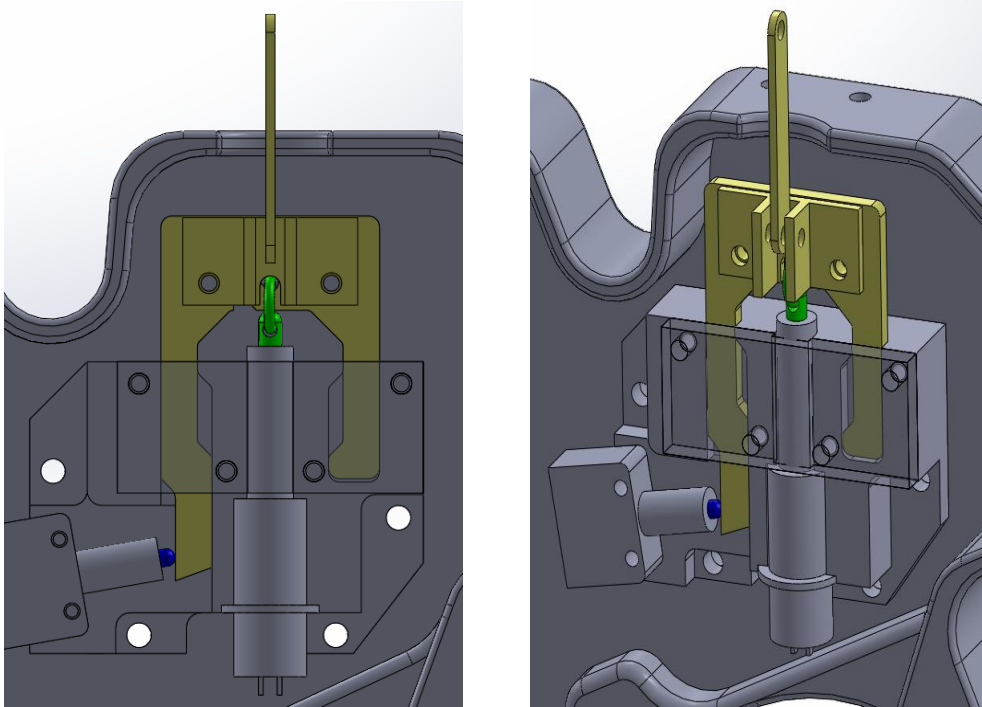


Figure 1: Current Slider Design

Preliminary Designs

After visiting our client's facilities, our team was refocused to address the complexity of the internal battery slider assembly. Two of the early designs considered can be found in Figures 2 and 3.

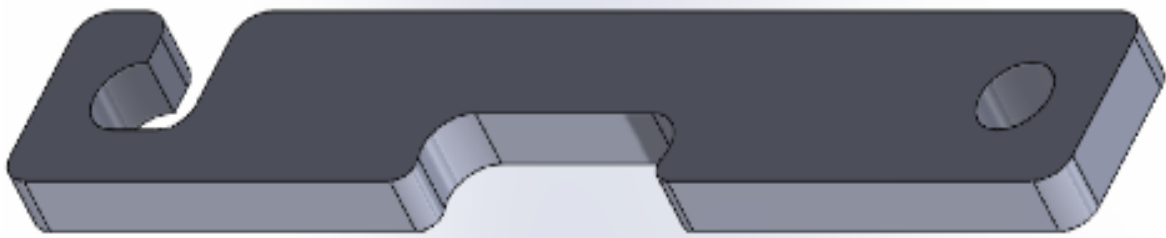


Figure 2: Slider Design 1

The primary difference between these designs and the current slider was the switch location and the surface area. With a smaller, more compact slider the internal complexity decreased as a result.

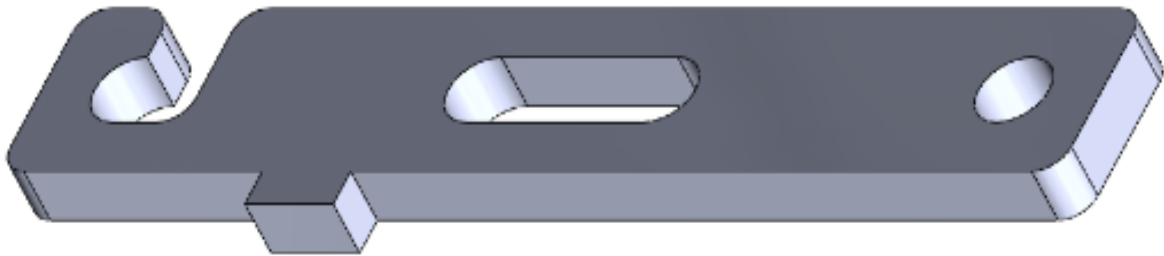


Figure 3: Slider Design 2

Design Analysis and Modifications

The newly designed assembly had certain criteria which needed to remain constant. The battery location on the assembly of the weapon was modeled as fixed features while the rest of the assembly could be moved for modifications. When taking into account these factors for the new assembly, the team came up with a new design to accommodate the constraints. A few factors came into consideration, such as having fewer parts, shorter machining and assembly time, easy to install, lower material cost, and overall less surface area for ice buildup. The angle of the switch which is currently placed at 10 degrees was mimicked to facilitate easier analysis. This affected where the switch could be placed, which imposed some constraints to where assembly components could be positioned in the new design.

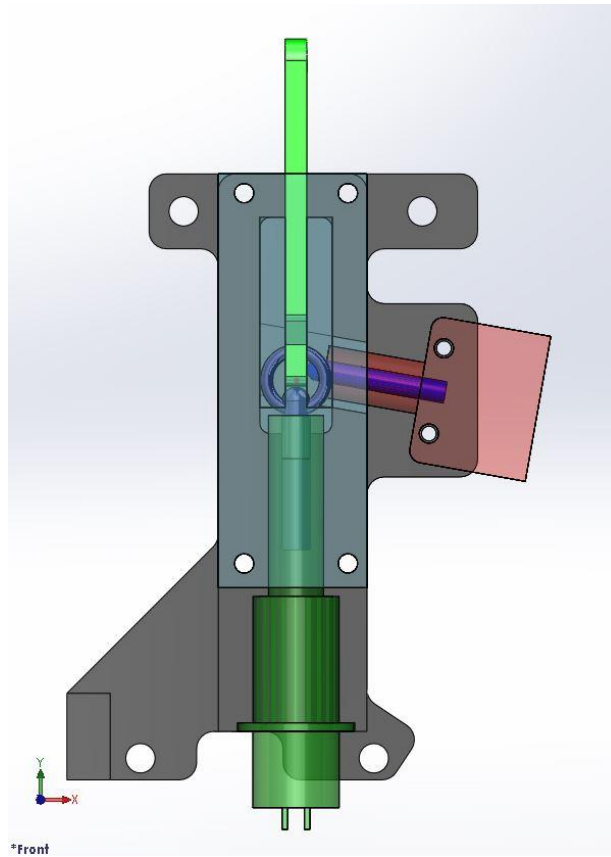


Figure 4: New Design Concept

The switch location for the new design was placed in the void area to the right of the current design (Figure 1). The location of the switch cavity paired with a single link/slider determined that the switch needed to be placed in a location close to the battery pull pin. As seen in Figure 4, the ideal location was found to be along the same line of action as the battery pull pin. With the switch mounted above the slider, interference with adjacent features was eliminated. The placement of the switch between the slider and the mount was deemed the best fit for a new design.

By taking these considerations into account, along with the dimensions of the switch, the location of the switch was determined to be approximately 0.75 inches above the battery as seen in Figure 4. The new location of the switch eliminated potential modifications to the base plate as well as the current weapon rib. As requested by Raytheon, the base plate for the new design was extended a half inch higher from the mounting location on the rib. This facilitated a smoother transition of the force from the outside of the weapon to the inside assembly.

The reduction in material, surface area, and mechanical components created a more reliable and efficient design. The improvements from the current design can be seen in the Table 2.

Table 2: Current vs. New Design Properties

	Current Design	New Design	Reduction (%)
Volume (in ³)	5.50	5.36	-2.55
Mass	0.21	0.21	-0.28
S.A. (in ²)	63.22	58.84	-6.93
Concerning S.A. (in ²)	11.48	6.74	-41.29
Mechanical Components	64.00	52.00	-18.75
Assembly Operations	6.00	4.00	-33.33
Machining Hours	2.60	2.10	-19.23
Machining Costs (\$)	200.00	150.00	-25.0

Two parts were removed from Raytheon’s current design which in turn eliminated 12 hardware components. This along with a 41% reduction in surface area was an immense improvement upon the current design.

New Base Plate Design

In redesigning the base plate, the team looked into minimizing the surface area and complexity of the activation system which resulted in a more compact base as seen in Figure 5.

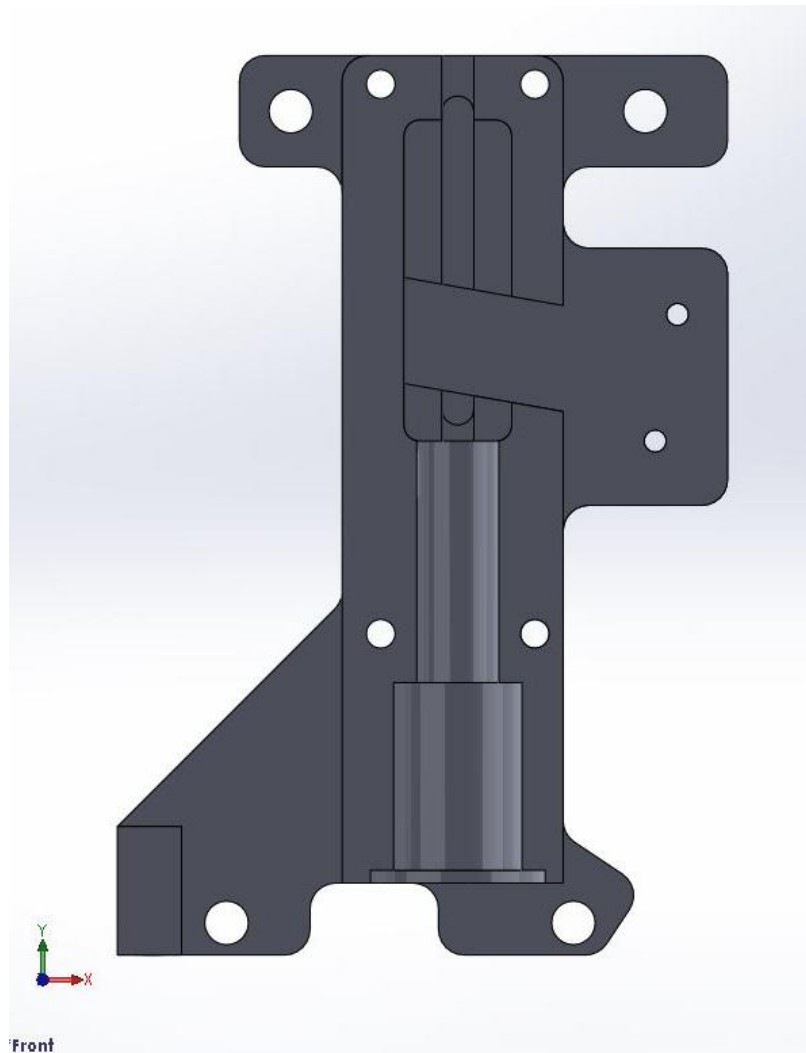


Figure 5: New Base Plate Design

This not only reduced the surface area and complexity of the system, but also eliminated two pieces in the manufacturing process. The new base plate also eliminated two screw types which will reduce confusion during assembly and installation time.

Material selection

The material chosen was AL6061-T6 due to its properties at cold and hot temperatures. It is required that this device is able to operate and withstand a temperature range of -51°C to 93°C (-60°F to 200°F). Figure 6 below, indicates AL6061 yield strength values at various temperatures above room temperature.

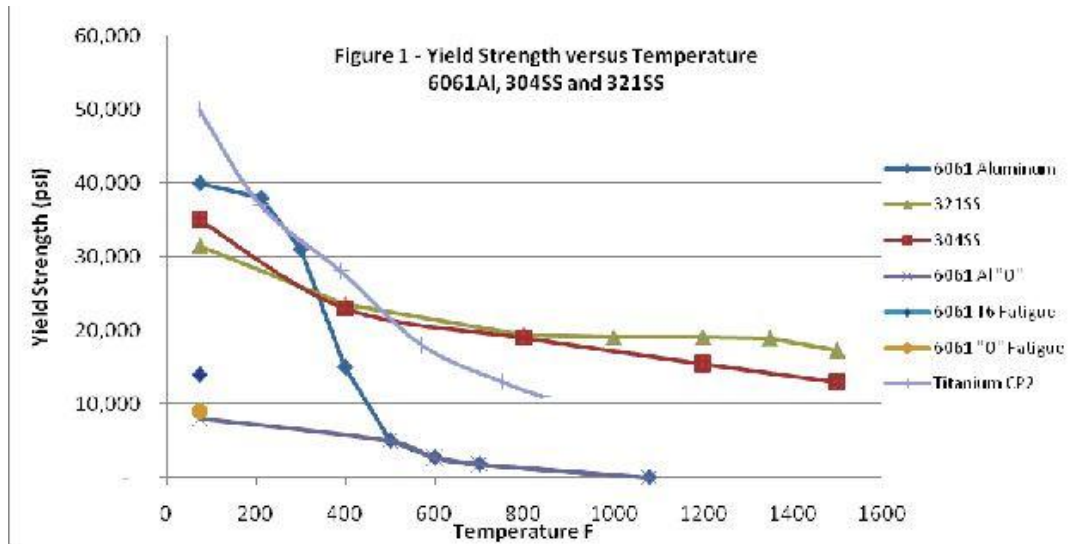


Figure 6: AL6061 Yield Strengths vs. Temperature [4]

As Figure 6 indicates, the yield strength of AL6061 drops with increasing temperatures. This lower yield strength was considered in our design decisions. Another material which was considered was steel. However, due to the temperature range exhibited by the device, steel was eliminated since it becomes very brittle at cold temperatures. Aluminum actually increases in yield strength at colder temperatures as indicated by Figure 7.

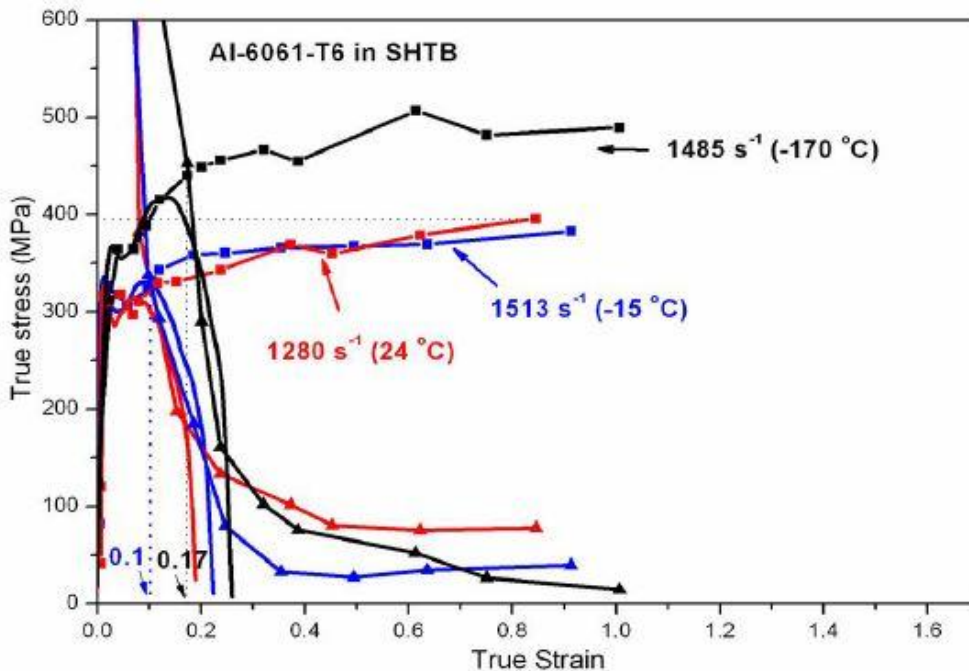


Figure 7: AL6061 True Stress vs. True Strain at Room Temperature to -170°C [3]

Top Designs

After receiving various dimensions needed to design the new slider and base plate, the previously mentioned slider designs were reconsidered and redesigned, which resulted in the slider seen in Figure 8.

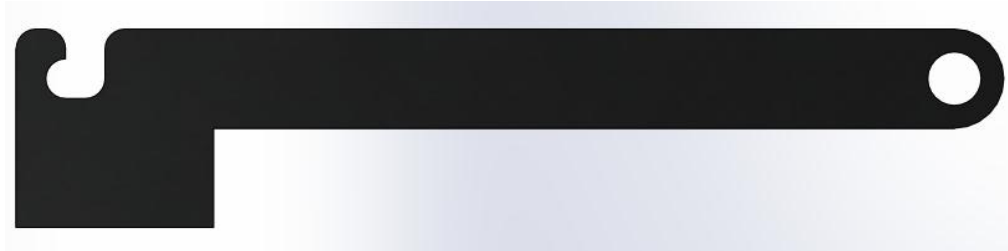


Figure 8: Slider Design 3

This design raised many concerns about its ability to perform the necessary tasks. To determine the performance of this design finite element analysis (FEA) was utilized. The FEA results of the applied force of 60lbs, at the hook of the slider, can be seen in Figure 9.

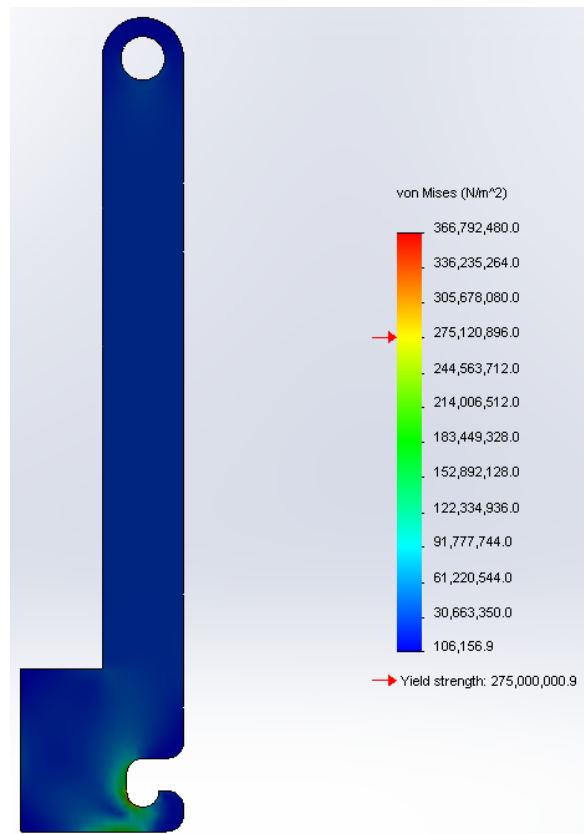


Figure 9: FEA of Slider Design 3

Figure 9 was computed considering AL6061-T6 with yield strength of 275 Mega-Pascals (MPa). Noticing that the stresses exhibited by the slider would be well above yielding, it was decided to double the thickness and adjust the geometry of the slider. The resulting design can be seen in Figure 10.

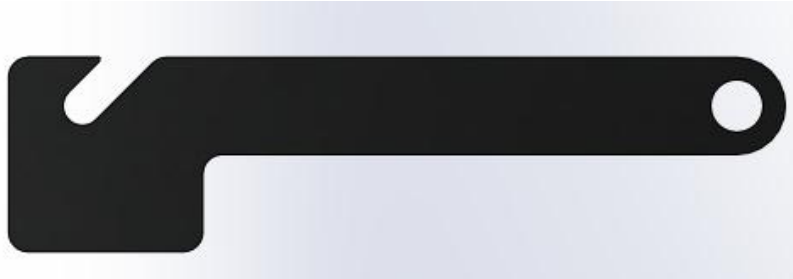


Figure 10: Top Design 1

After performing FEA on the new design, the results can be seen below, the maximum stress experienced by the slider dropped from 366MPa to 90.45MPa.

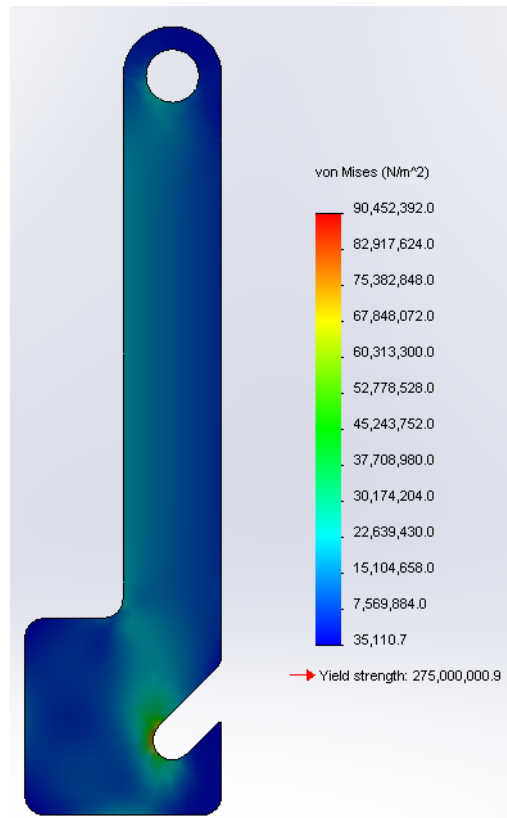


Figure 11: Top Design 1 FEA Analysis

The resulting factor of safety for this design was approximately 3. This newly designed slider was then placed in an assembly to get an idea of how the assembly as shown in Figure 12 below.

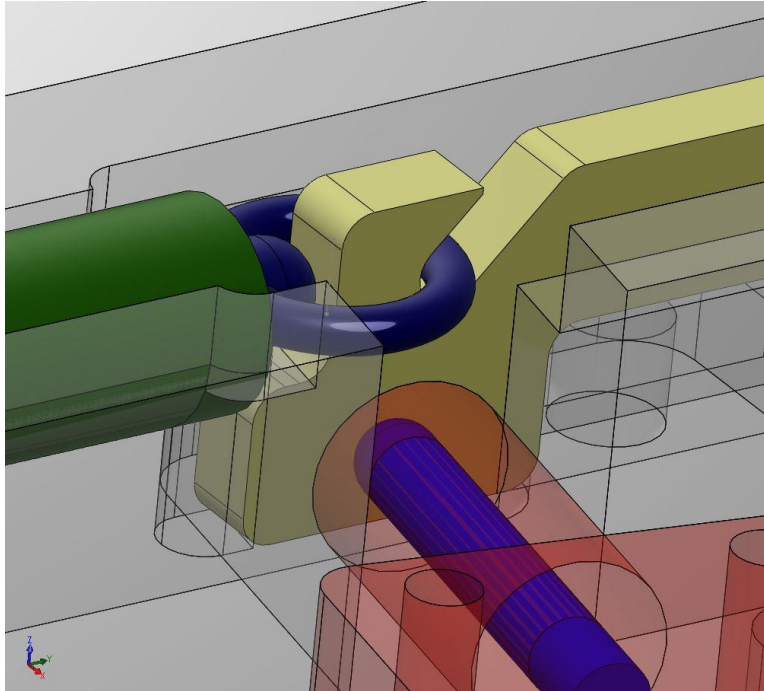


Figure 12: Slider Assembly Design

Based on the orientation of the slider and switch components, it was decided to consider an extended tab for the activation pin to rest on. This altered design can be seen in Figure 13. This extended tab creates more area for the activation pin to grip onto incase vibrations or other anomalies caused the slider to move out of place prematurely.



Figure 13: Top Design 2

Figure 14 below displays the results of the finite element analysis performed on this new slider design. These results indicate no significant change in stress concentrators, but slightly reduced the factor of safety to 2.64.

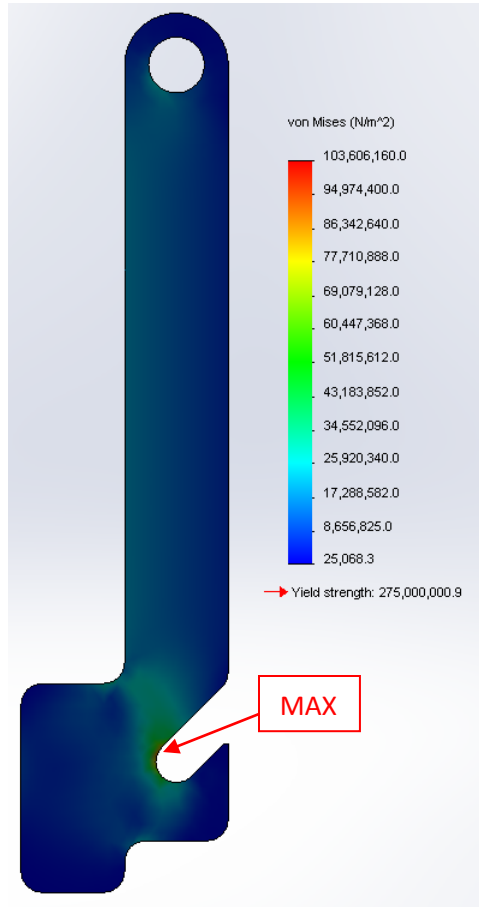


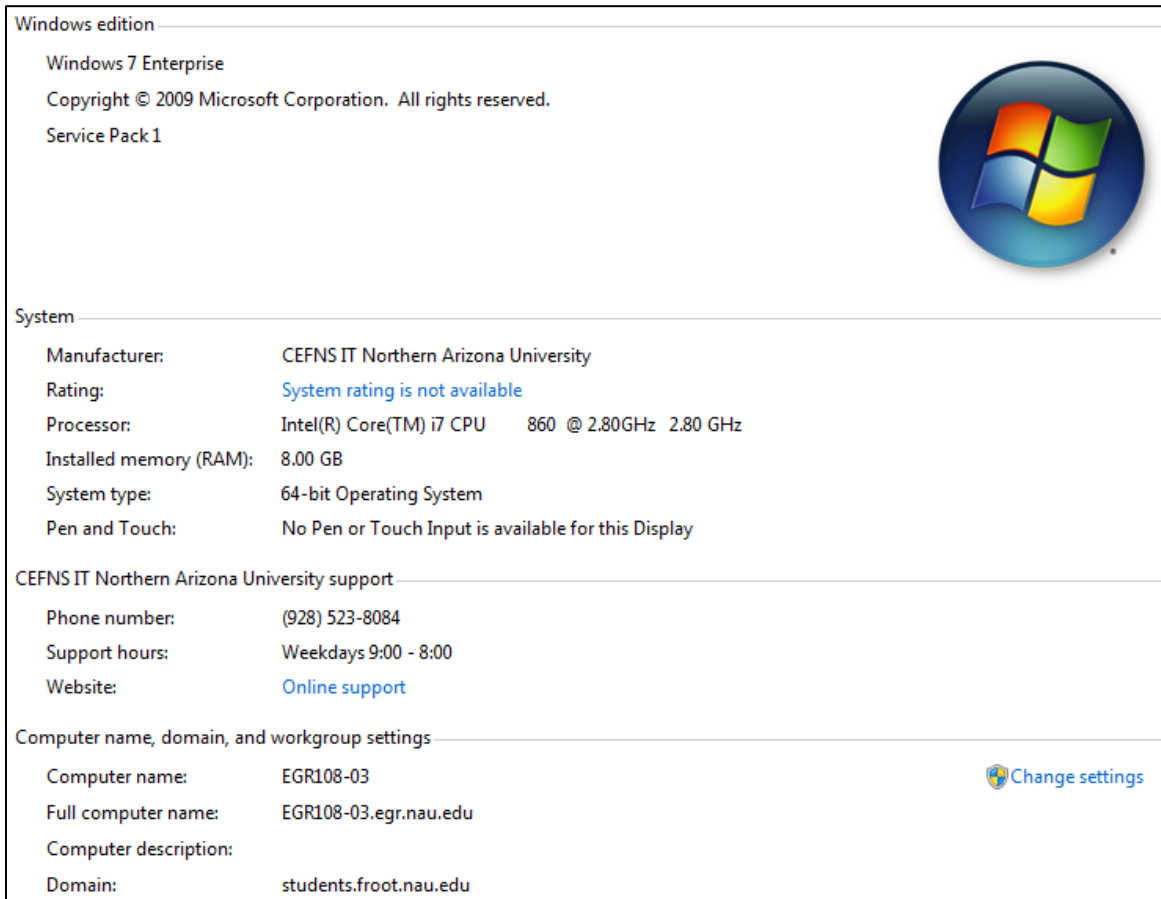
Figure 14: Top Design 2 FEA Analysis

When performing the FEA analysis, several trial runs were performed. The table below shows how various mesh sizes within the SolidWorks range option resulted in different

Table 3: Varying Mesh Sizes


	von Mises (Mpa)	Number of Nodes	Number of Elements	Element Size	Tolerance	% difference
Very Coarse	94.998816	2264	1161	0.08355	0.00417753	
						8.12629384
0.25	103.401528	4667	2632	0.062663	0.00313315	
						0.197509492
0.5	103.60616	12278	7447	0.0417753	0.00208877	
						0.996398624
0.75	104.64888	24487	15392	0.0318537	0.00159268	
						4.126090757
Very Fine	109.152616	80599	53782	0.0208877	0.00104438	

maximum von Mises stress. In order to determine which one to us, we calculated the percent difference between each trial. It was determined that the mesh size containing 12278 nodes and 7447 elements was the most ideal mesh. The time required to complete the mesh was 00:00:04 (hh:mm:ss). Figure 15 contains the detailed information on the computer system utilized for these analysis.



Windows edition

Windows 7 Enterprise
Copyright © 2009 Microsoft Corporation. All rights reserved.
Service Pack 1



System

Manufacturer: CEFNS IT Northern Arizona University
Rating: [System rating is not available](#)
Processor: Intel(R) Core(TM) i7 CPU 860 @ 2.80GHz 2.80 GHz
Installed memory (RAM): 8.00 GB
System type: 64-bit Operating System
Pen and Touch: No Pen or Touch Input is available for this Display

CEFNS IT Northern Arizona University support

Phone number: (928) 523-8084
Support hours: Weekdays 9:00 - 8:00
Website: [Online support](#)

Computer name, domain, and workgroup settings

Computer name: EGR108-03 [Change settings](#)
Full computer name: EGR108-03.egr.nau.edu
Computer description:
Domain: students.froot.nau.edu

Figure 15: Top Design 2 FEA Analysis

It was then decided to run the same analysis on the weakest link of the current slider switch to analyze the current maximum stress and factor of safety that it is experiencing. The resulting FEA model can be seen in Figure 16.

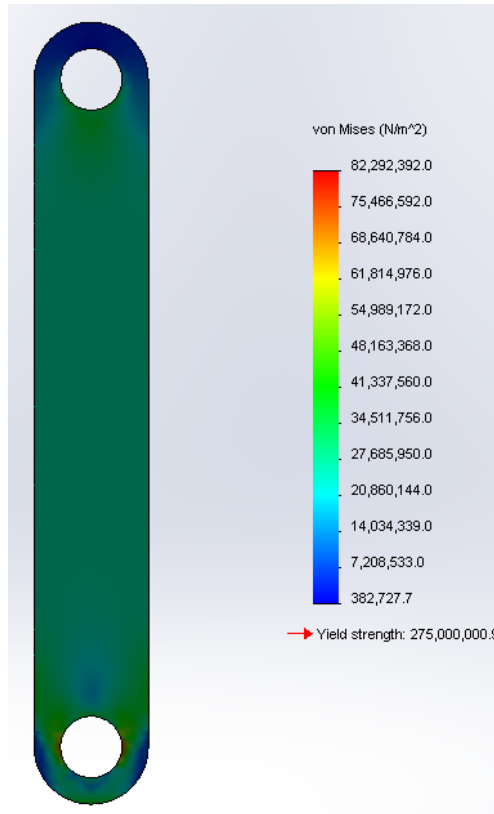


Figure 16: FEA of Weakest Link in Current Slider Design

The maximum stress experienced in the weakest link of Raytheon's design was 82MPa which resulted in a factor of safety of approximately 3. Our ultimate goal was to address all the issues experienced by the current design while maintaining this factor of safety. Based on the results above, the two top slider designs were considered for manufacturing. However, slider design 2 was selected after an experimental test to observe switch contacts. Figure 17 displays the assembly of this slider design and the accompanying baseplate.

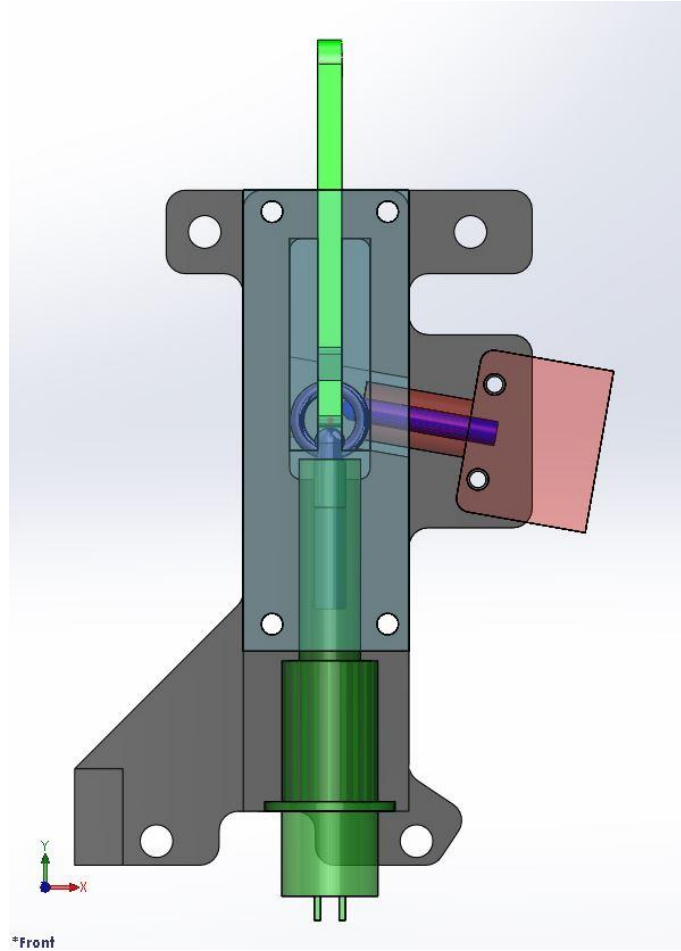


Figure 17: Top Slider 1 Assembly

Testing

Testing was performed using the weighted pulley system shown in Figure 18. The weight was used to mimic the forces seen by the system during activation. The red and green LEDs were used to indicate successful activation. During testing, three types of trial conditions were imposed using varying weights. These conditions include: no icing, moderate icing, and heavy icing. The heavy icing condition would be a worst case scenario which the device should never experience in actual conditions. These conditions were created through the use of a large freezer and a misting spray of water. Pictured below are the freezing orientations which created the moderate and heavy icing.

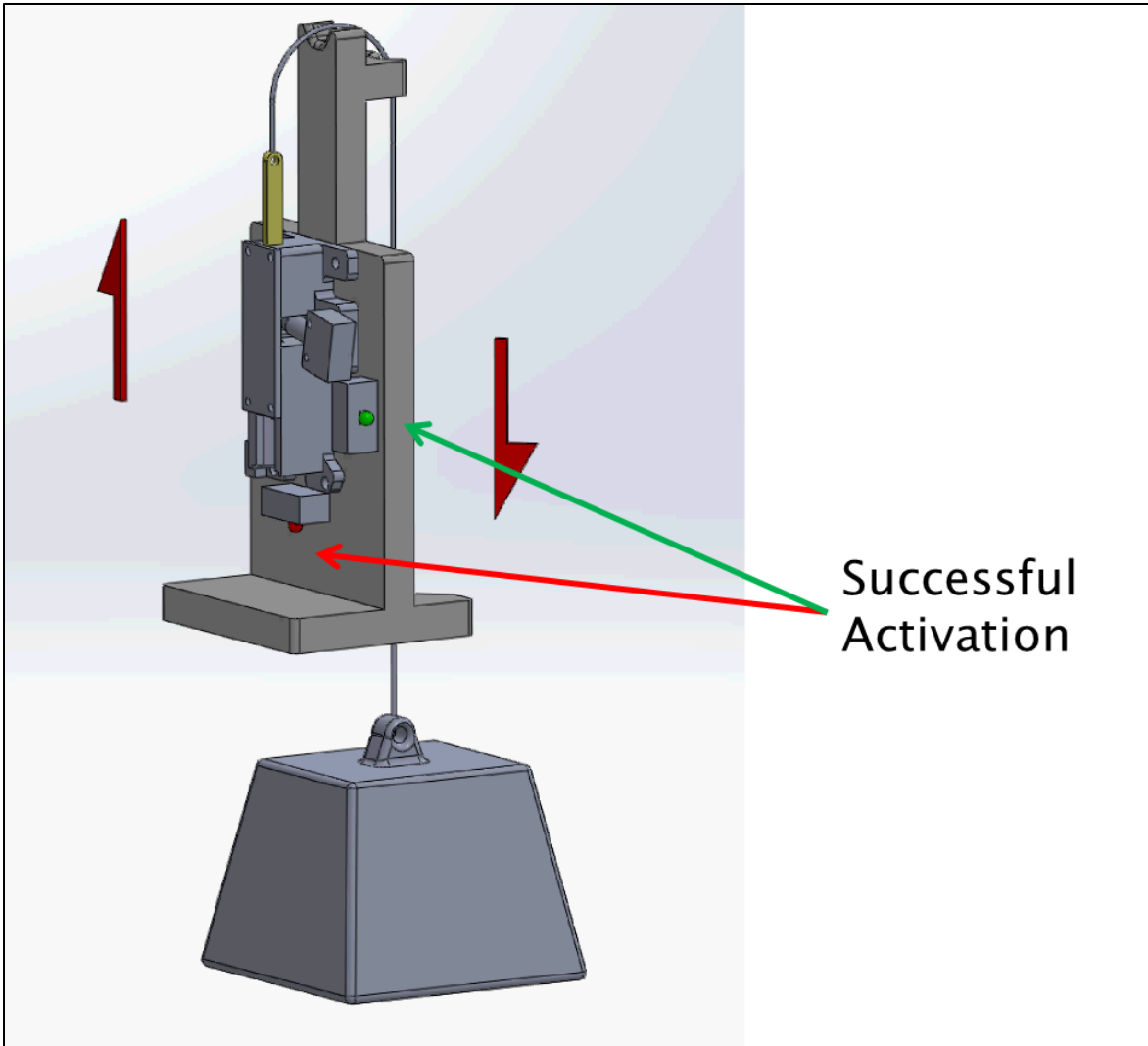


Figure 18: Experimental Setup

Displayed below are examples of the moderate and heavy icing using colored water to identify contamination regions.

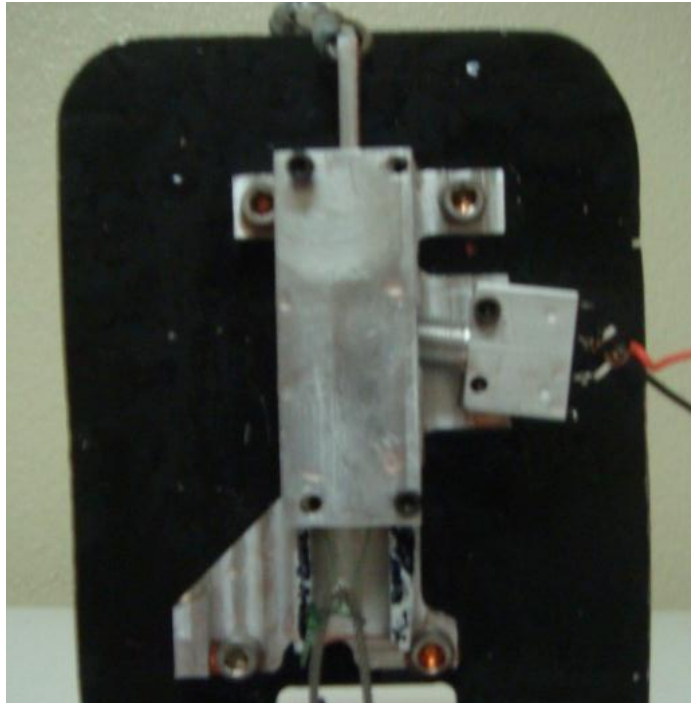


Figure 19: Vertical Freezing Orientation (resulted in moderate icing)

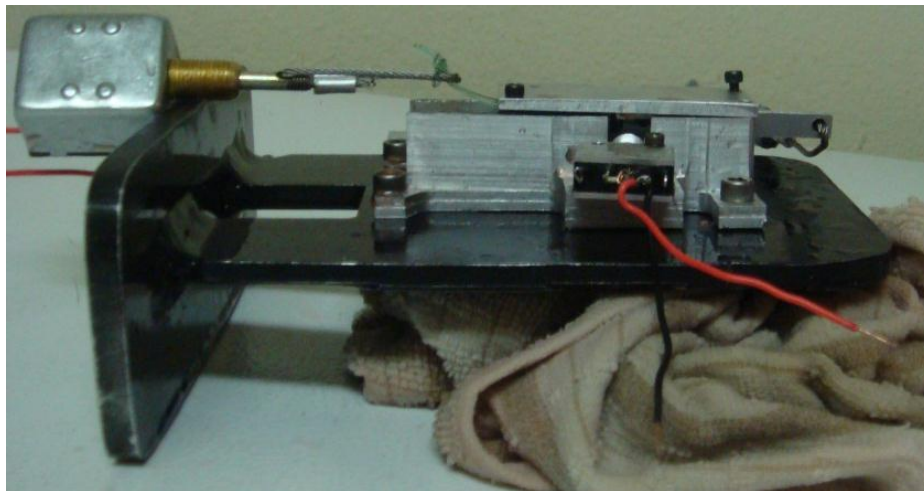


Figure 20: Horizontal Orientation (resulted in heavy icing)

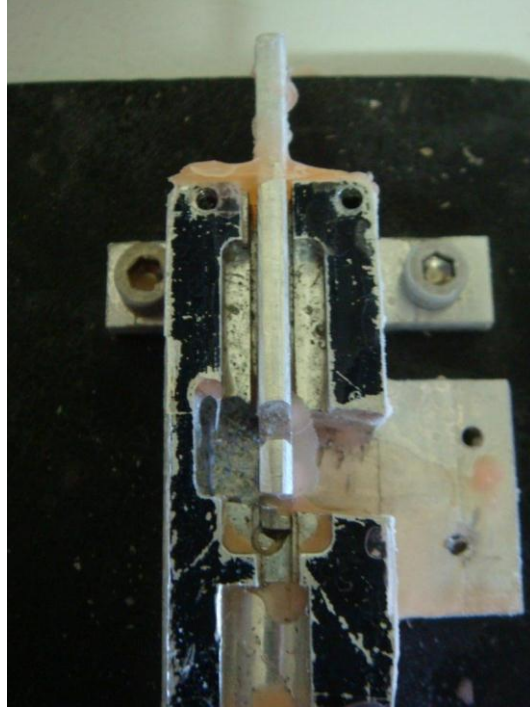


Figure 21: Example of Moderate Icing with Vertical Freezing Orientation

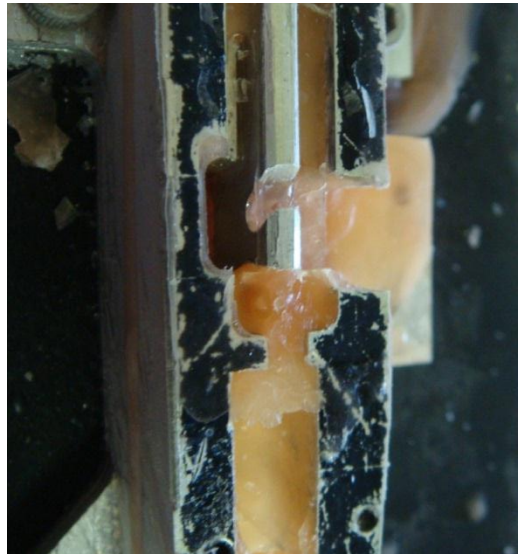


Figure 22: Example of Heavy Icing with Horizontal Freezing Orientation

The testing results pictured in Table 4 show successful or unsuccessful activation attempts for each of the three trial conditions. Based on the client's force requirements and accounting for a battery counter weight, the table below shows that the new device successfully activated under the required loads.

Table 4: Testing Results Using Varying Weights and Icing Conditions

	No Ice Build-up	Moderate			Heavy		
Weight (lbs.)	1	1	2	3	1	2	3
35	Pass	Fail	Pass	Fail	Fail	Fail	Fail
40	Pass	Pass	Fail	Fail	Fail	Fail	Fail
45	Pass	Pass	Fail	Fail	Fail	Fail	Fail
50	Pass	Pass	Fail	Pass	Pass	Pass	Fail
55	Pass	Pass	Pass	Pass	Pass	*Fail*	Fail
60	Pass	Pass	Pass	Pass	Pass	Pass	Pass

One case indicated by *Fail* was an anomaly where the slider activated successfully while the switch failed to activate due to ice buildup. The results of this test can be seen in Figure 23.

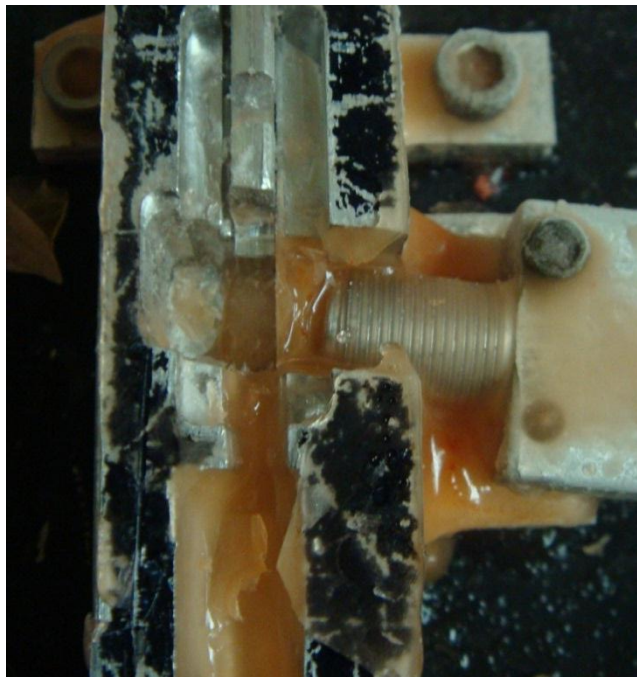


Figure 23: *Fail* Case Due to Switch Icing

Project Plan

The Gantt Chart in Figure 24 shows how the team planned to use the remainder of the semester's time. The black diamonds are milestones that represent the dates of presentations and report due-dates. Prototyping and early testing of the design was completed by mid-April.

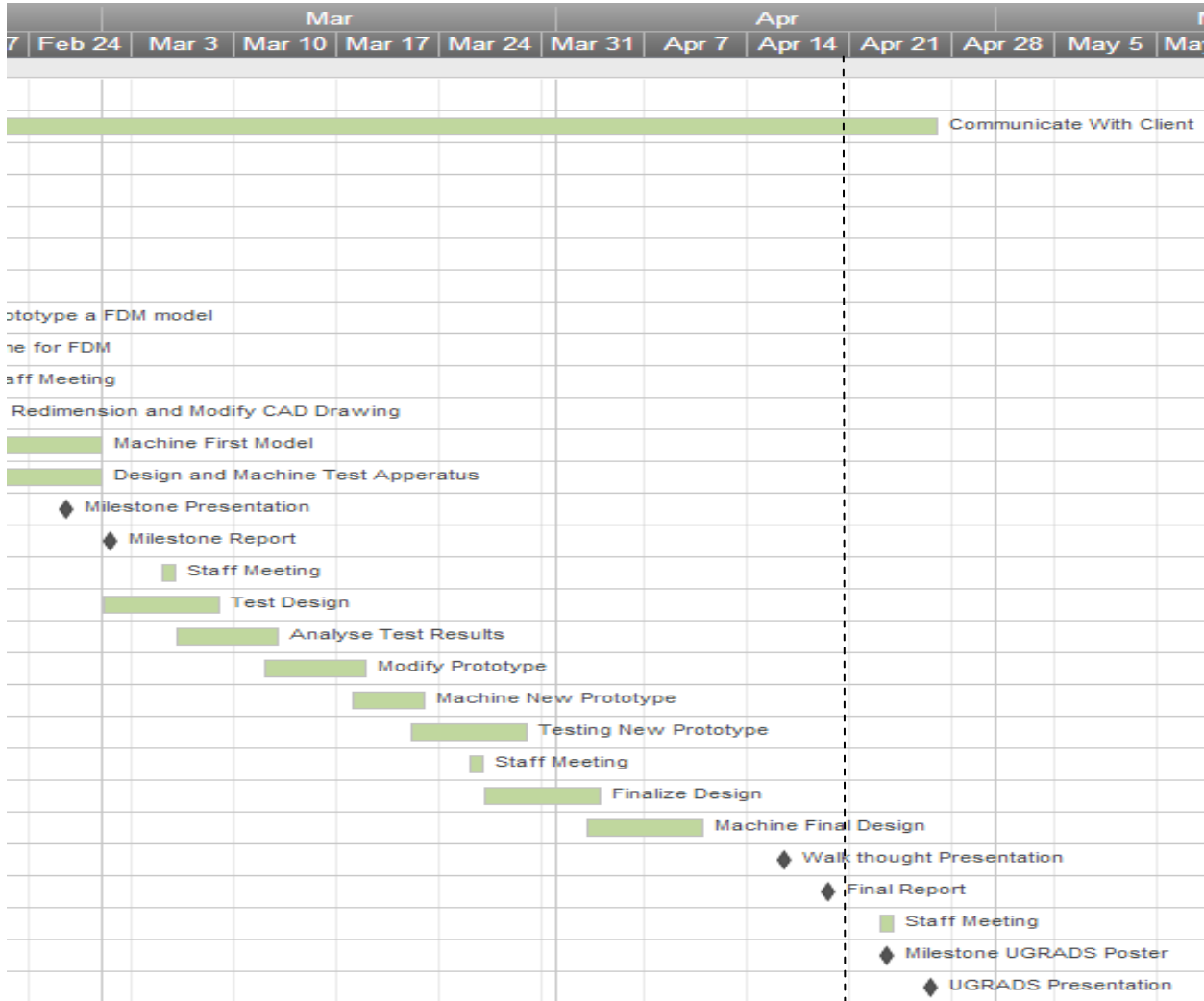


Figure 24: Gantt Chart for Spring 2013

Conclusion

The activation system used within Raytheon's weapons was experiencing failure due to icing, poor installation, and contaminants such as sand and dust. Raytheon requested our team to find a new design that was more reliable and less susceptible to these modes of failure. The activation slider that the team has designed reduced cost, reduced build time, reduced surface area, and reduced the number of components. Tables 2 and 4 reveal that

the failure percentage, time to assemble, and cost of manufacturing should decrease as a result. After undergoing our experimental failure contamination, this design surpassed expectations.

References

1. Chang, Tien, and Richard A. Wysk. *Computer-aided manufacturing*. 3rd ed. Upper Saddle River, NJ: Pearson Prentice Hall, 2006. Print.
2. "Raytheon Company: History." *Raytheon Company: Customer Success Is Our Mission*. N.p., n.d. Web. 7 Dec. 2012. <http://www.raytheon.com/ourcompany/history/>
3. Tang, Xin, VikasPrakash, and John Lewandowski. "Dynamic Tensile Deformation of Aluminum Alloy 6061-T6 and 6061-OA." n.pag. Web. 28 Feb 2013. <<http://sem-proceedings.com/06s/sem.org-2006-SEM-Ann-Conf-s11p02-Dynamic-Tensile-Deformation-Aluminum-Alloy-6061-T6-6061-OA.pdf>>.
4. "Yield Strength." *Burns Stainless*. N.p.. Web. 28 Feb 2013. <<http://www.burnsstainless.com/yieldstrength.asp&xgt;>>.